Diabetology & Metabolic Syndrome

RESEARCH

Open Access

Identification and regulatory mechanism analysis of macrophage-related key genes in diabetic nephropathy

Haijiao Wang[1], Li Zhang[1], Baochang Shi[2], Hao Li[1], Yan Liu[1] and Lei Zhu[1*]

Abstract

Background Diabetic nephropathy (DN) has been pathophysiologically associated with macrophage activity; however, the molecular mechanisms underlying this relationship remain unclear. This study aimed to explore the regulatory mechanisms linking DN and macrophages using integrated bioinformatics and experimental validation.

Methods The DN datasets were obtained from the Gene Expression Omnibus (GEO) database. Differentially expressed genes (DEGs) were identified by comparing DN samples with controls. Weighted gene co-expression network analysis (WGCNA) was performed to identify macrophage-related modular genes, which were intersected with DEGs to obtain differentially expressed macrophage-related genes (DE-MRGs). Key genes were screened using protein–protein interaction (PPI) analysis, least absolute shrinkage and selection operator (LASSO) regression, and support vector machine–recursive feature elimination (SVM-RFE). Single-cell RNA sequencing was applied to evaluate the expression of key genes at the single-cell level. Functional enrichment, immune infiltration, and drug correlation analyses were subsequently conducted. Finally, animal models were constructed to validate gene expression using RT-qPCR.

Results Four pivotal genes—LUM, FBN1, COL15A1, and LOX—were identified as significantly associated with immune cell infiltration, particularly macrophages and myeloid dendritic cells. The transcription factor FOXC1 was predicted to regulate all four key genes simultaneously. RT-qPCR confirmed that LUM, FBN1, and COL15A1 expression levels were markedly elevated in DN rat models compared with controls, consistent with bioinformatics findings.

Conclusions This study identified four macrophage-related key genes (LUM, FBN1, COL15A1, and LOX) closely associated with the pathogenesis of diabetic nephropathy. These findings provide novel insights into the immunoregulatory mechanisms of DN and potential therapeutic targets for future research.

Keywords Diabetic nephropathy, Macrophages, Bioinformatics analysis, Immune infiltration, Regulatory mechanism, Key genes

*Correspondence:
Lei Zhu
july200412@sohu.com
[1]Department of Endocrinology, Shandong Provincial Third Hospital,Shandong University, Jinan 250021, Shandong, China
[2]Department of Hepatobiliary Surgery, Shandong Provincial Third Hospital,Shandong University, Jinan 250021, Shandong, China

Introduction

As reported by the International Diabetes Federation, there were 537 million individuals with diabetes globally in 2021, with projections estimating this number to rise to 783 million by 2045 [1]. Diabetes and its complications have become major diseases that pose a serious threat to human health. Diabetic nephropathy (DN) represents one of the most prevalent and severe chronic microvascular complications arising from diabetes, progressively leading to a decline in renal function and potentially resulting in end-stage renal disease (ESRD) [2]. The pathological and physiological interaction between DN and ESRD further increases the complexity and difficulty of disease management [3]. Currently, the traditional standard treatment strategies for DN include controlling blood sugar and blood pressure, using renin-angiotensin system inhibitors, managing lipids, and promoting weight loss [4]. In recent years, mineralocorticoid receptor antagonists [5], SGLT-2 inhibitors [6], and GLP-1 receptor agonists [7] have shown renoprotective effects in clinical trials. However, even such comprehensive treatments cannot completely prevent the progression of DN to ESRD, and the prevalence of DN among diabetic patients has remained largely unchanged in the past decade [3]. Meanwhile, due to the characteristics of this disease such as its insidious onset, low awareness, and high rate of misdiagnosis [8], the early diagnosis and prevention and treatment of this disease face significant challenges. Therefore, early detection and identification of novel key genes associated with DN are essential for timely intervention, significantly enhancing the prognosis for DN patients.

Recent investigations have highlighted that exudation of inflammatory cells and overexpression of pro-inflammatory cytokines are key pathogenic mechanisms in DN [9]. Among them, the migration of monocytes/macrophages to the renal tissue and the dynamic changes in their polarization state (M1/M2 phenotypes) play a crucial role in the development of DN [10–11]. Renal biopsies taken from patients across all stages of DN have consistently demonstrated the presence of macrophages within the interstitial and glomeruli. Hyperactivated macrophages release a substantial quantity of inflammatory cytokines, exacerbating the inflammatory response of intrinsic renal cells, extracellular matrix secretion, fibrosis, and necrosis. Targeting macrophages for depletion and inhibiting the Notch pathway in macrophages can alleviate pathological changes in renal cells [12]. Although the importance of macrophages in the occurrence and development of DN has been widely recognized, the specific mechanism remains unclear, especially there is a lack of systematic research based on multi-omics integration. This limits the further development of early diagnosis and targeted treatment strategies for DN.

This study was based on transcriptomic data from 41 DN patients and 20 normal controls in the Gene Expression Omnibus (GEO) database. Through differential gene expression analysis and machine learning, we comprehensively explored the expression, function, immune infiltration, and molecular regulation of MRGs. This research aimed to reveal the potential roles and molecular mechanisms of DN, and validation was conducted in animal models to provide novel insights into clinical diagnosis and treatment approaches. In particular, the application of scRNA-seq technology has been applied to reveal the transcriptomic characteristics of different cellular subpopulations, further deepening our understanding of the cellular heterogeneity and potential pathological processes in DN. It has also clarified the roles of key genes in various cell subpopulations, providing new insights into the pathological mechanisms of DN.

Materials and methods

Data source

Three datasets related DN (GSE96804, GSE142025 and GSE131882) were sourced from the GEO database (https://www.ncbi.nlm.nih.gov/gds). Tissue samples from glomerular and renal biopsies were utilized in GSE96804 (GPL17586) and GSE142025 (GPL20301) datasets, which contained 20 and nine control and 41 and 27 DN patients (Case), respectively. Moreover, the GSE131882 dataset (single-cell RNA sequencing (scRNA-seq), GPL24676) included three control and three case samples (kidney tissue).

Immune infiltration analysis and weighted gene co-expression network analysis (WGCNA)

To enhance our understanding of immune cell infiltration in the GSE96804 dataset, we evaluated the differences in the abundance of 36 immune cell types between the two groups using a single-sample Gene Set Enrichment Analysis (ssGSEA)-based approach, specifically employing the XCell immunedeconv computational tool (version 2.1.0) [13]. Next, samples in the GSE96804 dataset were clustered using the full function of the WGCNA program (v1.71) [14] in order to eliminate outlier samples. Subsequently, the optimal soft threshold (β) was selected in the co-expression network to approach a scale-free distribution. After that, a cluster dendrogram was constructed using adjacency and similarity calculations. By establishing a minimum module size of 100 for the genes dendrogram, a dynamic tree cutting technique was employed to acquire modules. The key modules identified exhibited a strong positive correlation with macrophages, M1 macrophages, and a high negative correlation with M2 macrophages, or conversely, a high negative correlation with macrophages and M1 macrophages alongside a strong positive correlation with M2 macrophages ($|R|>0.3$ and P

< 0.05). Ultimately, the genes within these modules were designated as modular genes for subsequent analyses.

Identification of differentially expressed macrophage-related genes (DE-MRGs)

Initially, the limma package (v 3.52.4) [15] was implemented to evaluate DEGs across case and control groups in the GSE96804 dataset. The significance threshold was set at $|\log2FC| \geqq 1$ and p.adj < 0.05. The Benjamini-Hochberg method was employed to correct the p-values for multiple comparisons, thereby controlling the false discovery rate. The ggplot2 (v 3.3.6) and heatmap3 (v 1.1.9) were utilized to create volcano plots and heatmap revealing DEG expression [16, 17]. Finally, DEGs from case and control groups were merged with modular genes via UpSetR (v 1.4.0) to look for DE-MRGs in DN [18].

Chromosomal localization, protein-protein interactions (PPI) and Functional enrichment analyses in DE-MRGs

Chromosome localization analysis was carried out utilizing OmicCircos (v1.38.0) [19]to investigate the position of DE-MRGs in chromosomes. Meanwhile, DE-MRGs were subjected to Gene Ontology (GO) and Kyoto Encyclopedia of Genes (KEGG) analyses with the clusterProfiler package (v 4.4.4) (*p.adj* < 0.05) [20]. Additionally, through the Search Tool for Recurring Instances of Neighboring Genes database (STRING, https://string-db.org) [21], the PPI network of DE-MRGs was constructed. The interaction data was imported into the Cytoscape program (v 3.9.1) [22] for visualization. Furthermore, the impact of DE-MRGs was assessed by the following six techniques from the CytoHubba Plugin for Cytoscape: Maximum Clique Centrality (MCC), Maximum Neighborhood Component (MNC), Degree, Edge Percolation Component (EPC), Closeness and Radiality. The overlapping portion of the top20 for each algorithm was defined as candidate genes.

Least absolute shrinkage and selection operator (LASSO) and support vector machine-recursive feature elimination (SVM-RFE) screening for key genes

To obtain the key genes in GSE96804 dataset, we performed machine learning screening which was based on candidate genes. First, the glmnet package (v4.1-4) [23] was employed to conduct LASSO regression analysis on candidate genes. Optimal regularisation parameters were determined through five-fold cross-validation, with the gene set corresponding to the minimum cross-validation error (lambda.min) ultimately selected as the LASSO screening result. Concurrently, the e1071 package (v1.7-11) [24] was employed to implement Support Vector Machine Recursive Feature Elimination (SVM-RFE). Through an iterative process, genes contributing least to classification were progressively removed in each round, thereby refining the feature subset until the optimal gene combination was attained. Throughout this process, five-fold cross-validation was employed to systematically evaluate the classification performance of gene subsets at each stage, thereby ensuring the robustness and reliability of the selected gene combinations across varying data distributions. The resulting overlapped sections of the genes were designated as key genes. Then, the diagnostic effectiveness of the key genes was assessed by plotting receiver operating characteristic (ROC) curves for GSE96804 and GSE142025 datasets independently using the pROC software (v1.18.0) (area under curve (AUC) > 0.8) [25]. Additionally, groups in the two datasets were compared separately for the expression of key genes (P < 0.05). Spearman's correlation coefficient was calculated to explore the relationship between differential immune cells and key genes.

GSEA functional enrichment

GSEA enrichment analysis was performed to gain insights into the biological functions and signaling pathways associated with the key genes. To begin, correlations between key genes and other genes were calculated independently and ranked from high to low via Spearman in GSE96804 dataset. Following that, using the GSEA function, the sorted genes were enriched in the KEGG background set, which downloaded by msigdbr (v 7.5.1) (*p.adj* < 0.05) [26].

Single-cell RNA sequencing data pre-processing

The Seurat program (v 4.3.0) was utilized for data front-end processing and quality control on six samples that were derived from the GSE131882 dataset [27]. To summarize, genes that met the requirements of having at least three cells with expression data, having more than 200 detected genes (minimum number of cells = 3, minimum number of features = 200), and meeting additional thresholds of gene count within cells ≤ 4000, total gene expression counts ≤ 50,000, and mitochondrial gene expression ≤ 20%. After centralizing the data, the top 2000 (highly variable genes) with comparatively large intercellular coefficients of variation were selected using the vst method. The single-cell data were then integrated according to the common highly variable genes in each sample.

Cell clustering, annotation and expression assessment of key genes

Following the principal component inflection point charting and principal component analysis (PCA) replacement test, the JackStrawPlot function was also utilized to compare the distribution of p-values for each PC and the first 30 principal components (dims = 30) were chosen for data dimensionality reduction. And

unsupervised uniform manifold approximation and projection (UMAP) clustering analysis was performed on the filtered cells using the seurat package's FindNeighbors and FindClusters functions (resolution = 0.8). Finally, cellular annotation was accomplished using marker genes from the literature [28], following by an analysis of key gene expression differences between clusters.

Molecular regulation of key genes and drug prediction

To investigate the molecular regulatory mechanisms of key genes in DN, we built transcription factors (TFs)-mRNA and competitive endogenous RNA (ceRNA) networks. MiRNet (https://www.mirnet.ca/) was used to predict TFs (degree ≧ 1) related with key genes based on the JASPAR database. To discover the key genes that might ultimately govern the miRNAs and lncRNAs, it was first necessary to satisfy both PITA and miRmap databases predicted at the same time, as well as clipExpNum ≧ 10 and clipExpNum ≧ 20, respectively. Finally, potential drugs for key genes were obtained by analyzing in comparative toxicogenomics database (CTD; http://ctdbase.org/). Network visualization were using Cytoscape (v3.9.1) [22].

DN rat models construction

Male SD rats aged 6 to 8 weeks were split into two groups at random (DN and control, each with 5 rats). The rats were purchased from Spfbiotech Co., Ltd. (Beijing) (Production License No.: SCXK (Beijing) 2019-0010; Use License No.: SYXK (Yunnan) K2020-0006). All animal experiments received ethical clearance from the Ethics Committee of Shandong Provincial Third Hospital (ethical batch number: SYDW-SDLH-2024003) and were conducted in meticulous adherence to the Guide for the Care and Use of Laboratory Animals. Following eight weeks of control and high-fat, high-sugar chow feeding, the rats received intraperitoneal injections of 60 mg/kg streptozotocin (biosharp, BS185-100 mg) in the DN group and an equivalent quantity of saline in control group. Subsequently, we monitored body weight and blood glucose in each group of mice, as well as performed volume size measurements, Hematoxylin Erythropoietin (HE) staining, and quantitative reverse transcriptase polymerase chain reaction (qRT-PCR) assays on kidney tissues. At the experimental endpoint (8 weeks post-streptozotocin induction), rats were euthanized humanely. Animals were first anesthetized by intraperitoneal injection of pentobarbital sodium (40 mg/kg) to ensure unconsciousness (verified by lack of toe-pinch response and corneal reflex). Euthanasia was then performed via an overdose of pentobarbital sodium (100 mg/kg, intraperitoneal injection), inducing rapid cardiorespiratory arrest in accordance with AVMA Guidelines for the Euthanasia of Animals. Kidney tissues were immediately harvested for subsequent analyses, including HE staining and qRT-PCR.

HE staining

Kidney tissues were fixed in a 4% paraformaldehyde solution prior to undergoing dehydration, embedding, and sectioning.Following baking and deparaffinization, the tissues were rehydrated using an alcohol gradient. Staining was performed with hematoxylin for five minutes and eosin for a duration of 5 to 10 s, after which the samples were dehydrated, clarified, and sealed.

Quantitative reverse transcriptase polymerase chain reaction (qRT-PCR) detection of key genes

Using the TRIzol(invitrogen,15596018CN)reagent, RNA was extracted from each set of kindey tissue sample. The procedures included RNA precipitation, cleaning, dissolution, quality assessment, and sample cDNA synthesis. Transcript in reverse: 25 °C, 5 min; 55 °C, 15 min; 85 °C, 5 min. The key genes were amplified in accordance with the SweScript-First-strand-cDNA-synthesis-kit's (Servicebio,

G3336-50) instructions. Predenaturation at 95 °C for 5 min, denaturation at 94 °C for 10 s, annealing at 60 °C for 30 s, and 40 cycles comprised the amplification process. Using the $2^{-\Delta\Delta CT}$ technique, the expression of key genes for each sample was standardized to GAPDH. In Table S1, the primer sequence was displayed.

Statistical analysis

All bioinformatics analyses were executed using R software. The Wilcoxon test was employed to conduct comparisons between different groups. A p-value of less than 0.05 was deemed statistically significant.

Results

There were 8,935 modular genes related with macrophages in DN

In GSE96804 dataset, range of analyses were implemented to identify genes linked with macrophages. At the start, immune infiltration analysis revealed significant changes in the relative composition of 18 immune cells and 2 scores between case and control samples (Fig. 1A). Among these, neutrophils, M2 macrophages and T-helper type 1 (Th1) had larger content in control group than in the case group, nevertheless the remainder of the immune cells and scores exhibited opposite tendencies. Focusing on the three types of macrophages we discovered that M1 macrophages and macrophages were considerably higher in the case group, yet M2 macrophages were much lower (Fig. 1B).

Then, with three different types of macrophages as traits, we executed the WGCNA. The sample clustering findings demonstrated that there were no outlier samples

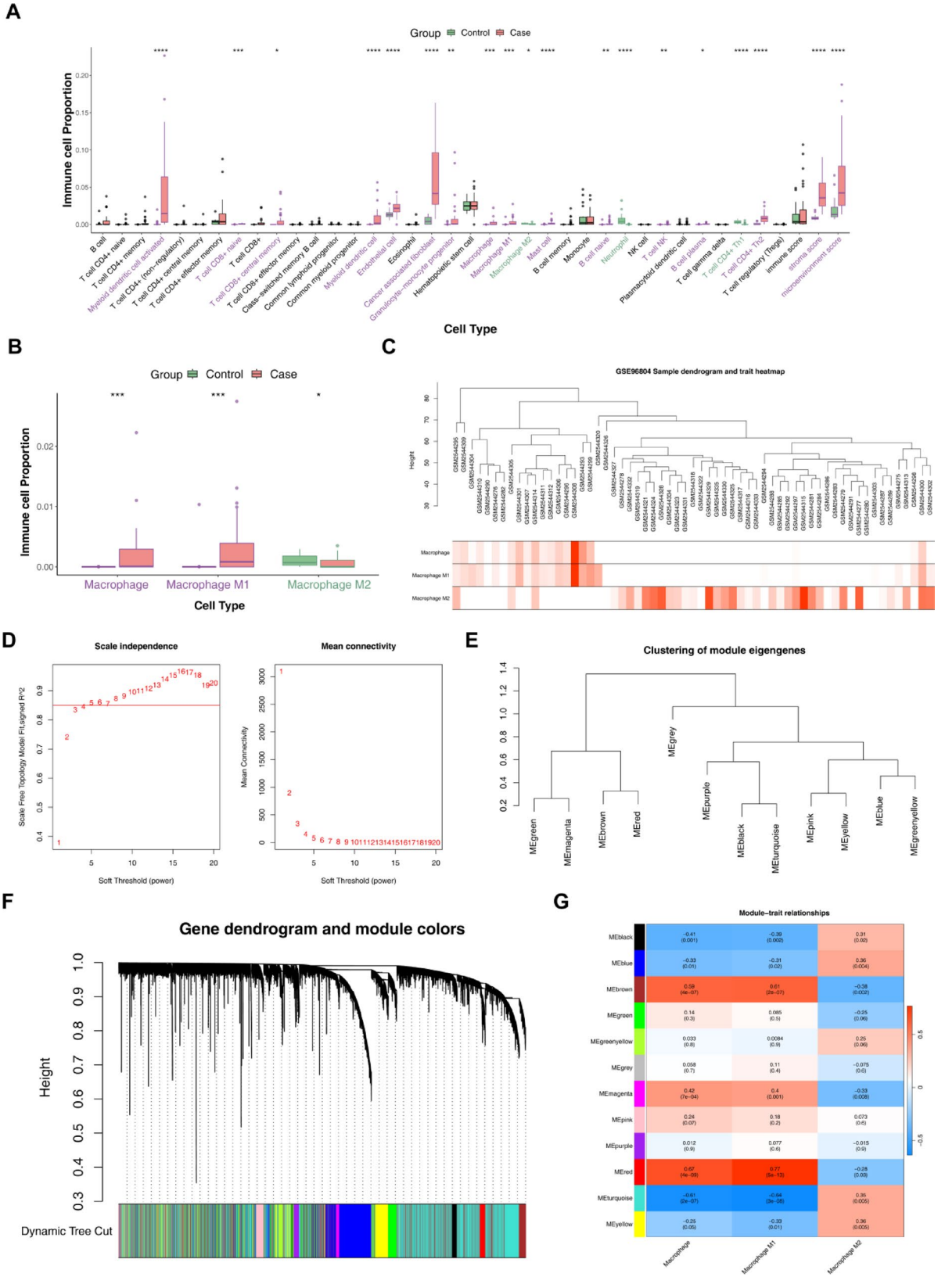

Fig. 1 Modular genes related with macrophages in DN. **A-B**. Immune infiltration analysis comparing the relative composition of 18 immune cells and two scores between case and control samples. **C**. Sample dendrogram and trait heatmap. **D**.Scale-free fit index and network connectivity under different soft thresholds. **E-F**. Clustering of module eigengenes and hierarchical clustering of genes. **G**. Heatmap showing the correlation between gene modules and macrophage characteristics.

(Fig. 1C). When the soft threshold was set to 6, interacting genes suited the scale-free distribution the best (Fig. 1D). The dynamic tree-cutting technique yielded a total of 12 modules (Fig. 1E and F). Modules MEbrown (2,399) and MEturquoise (6,536) were chosen as key modules, and 8,935 genes classified as module genes (Fig. 1G).

Autosomal-localized 127 DE-MRGs may be crucial regulators of DN

In the GSE96804 dataset, differential expression analysis yielded 644 DEGs when comparing case and control samples, consisting of 306 upregulated and 338 downregulated genes (Fig. 2A and B). Whereafter, DEGs between case and control groups were overlapped with 8,935 module genes, yielding 127 DE-MRGs (Fig. 2C).

The distribution of all 127 DE-MRGs in autosomes was revealed by Chromosomal localization (Fig. 2D). Then, in order to analyze the pathogenic and functional pathways of 127 DE-MRGs, GO and KEGG enrichment were examined. According to GO functional enrichment analysis, DE-MRGs were primarily enriched in collagen-containing extracellular matrix and external encapsulating structure organization (Fig. 2E). In accordance with the KEGG analysis, DE-MRGs were mainly abundant in AGE-RAGE signaling pathway, Chemokine signaling pathway and the PI3K-Akt signaling pathway, (Fig. 2F).

Ultimately, we looked for connections between the proteins corresponding to 127 genes, and observed among them, COL1A2-LUM and IGF1-IGFBP6 exhibited the greatest binding indices (Fig. 2G). Furthermore, after filtering by six algorithms of Cytoscape's cytoHubba plugin, we identified 15 genes that appeared in the top 20 of each algorithm and designated them as candidate genes (Fig. 2H).

LUM, *FBN1*, *COL15A1*, and *LOX* were key genes for DN

We subsequently employed machine learning algorithms to scan for key genes in DN. When lambda. min = 0.009, we acquire six feature genes and the LASSO error was minimized (Fig. 3A and B). Similar to this, we obtain eight feature genes at the point where the SVM-RFE model error was lowest (Fig. 3C). The intersection of feature genes from both machine learning methods yielded four key genes: LUM, FBN1, COL15A1, and LOX (Fig. 3D). Furthermore, the AUC values of the four key genes in the GSE96804 and GSE142025 datasets were all greater than 0.8, demonstrated that they had favorable diagnostic capabilities for DN (Fig. 3E and F). Meanwhile, gene expression was considerably distinct between groups and trended in the same direction, with *LUM*, *FBN1*, and *COL15A1* up-regulated and *LOX* down-regulated in the case group (Fig. 3G and H).

All of the key genes were involved in oxidative phosphorylation

Following a correlation analysis between differential immune cells and key genes, it was demonstrated that four key genes had a strong association with the following: macrophage, granulocyte-monocyte progenitor, activated myeloid dendritic cell, myeloid dendritic cell, and cancer linked fibroblast (Fig. 4A). Moreover, the key genes were primarily associated with oxidative phosphorylation and cytokine-cytokine receptor interaction, according to the GSEA enrichment data (Fig. 4B and E).

The 13 cell populations in the DN were determined by scRNA-seq

Following data normalization and filtering to eliminate low-quality cells and genes, a total of 25,733 genes and 22,667 cells were detected (Fig. 5A and S1-S8). Subsequently, PCA downscaling indicated the absence of outliers and abnormal cells (Figs. 5B and S9-S10). After UMAP clustering, it was discovered that all samples were classified into 22 clusters, which comprised 13 cell populations after maker gene annotation (Fig. 5C and D, Table S2). At last, our analysis of key gene expression in distinct cell populations revealed that *LUM* expression was elevated in the MES; *FBN1* expression was elevated in both the MES and ENDO; *COL15A1* expression was elevated in the ENDO; *LOX* expression was elevated in PODO expression (Fig. 5E).

FOXC1 was an essential TF that simultaneously regulates four key genes

Relevant regulatory networks were built in order to comprehend the molecular mechanisms by which key genes modulate DN. Initially, we identified 33 transcription factors (TFs), among which FOXC1 was an essential one that simultaneously regulates four key genes (Fig. 6A, Table S3). In addition, we built the ceRNA network, which included 37 lncRNAs, 27 miRNAs, and 4 key genes, such as *FBN1*-hsa-miR-362-3p-KCNQ1OT1, *LOX*-hsa-miR-876-5p-NEAT1 (Fig. 6B, Table S4). Lastly, we recognized 28 chemicals in the CTD database that we projected may either enhance the expression of LOX or reduce the expression of FBN1, COL15A1, and LUM. Among these, dexamethasone may have an effect on LOX, COL15A1, and LUM simultaneously (Fig. 6C, Table S5).

Remarkable structural changes to the kidneys in DN rats

To detect the expression of key genes, we created a DN rat model (Fig. 7A). The results showed that the rats in DN group began to weigh more than the control group on day 36, and following the streptozotocin intervention, the weight began to decline (Fig. 7B). Meanwhile, before the intervention, the blood glucose of both groups of mice stayed between 3 and 7 mmol/L, and after the

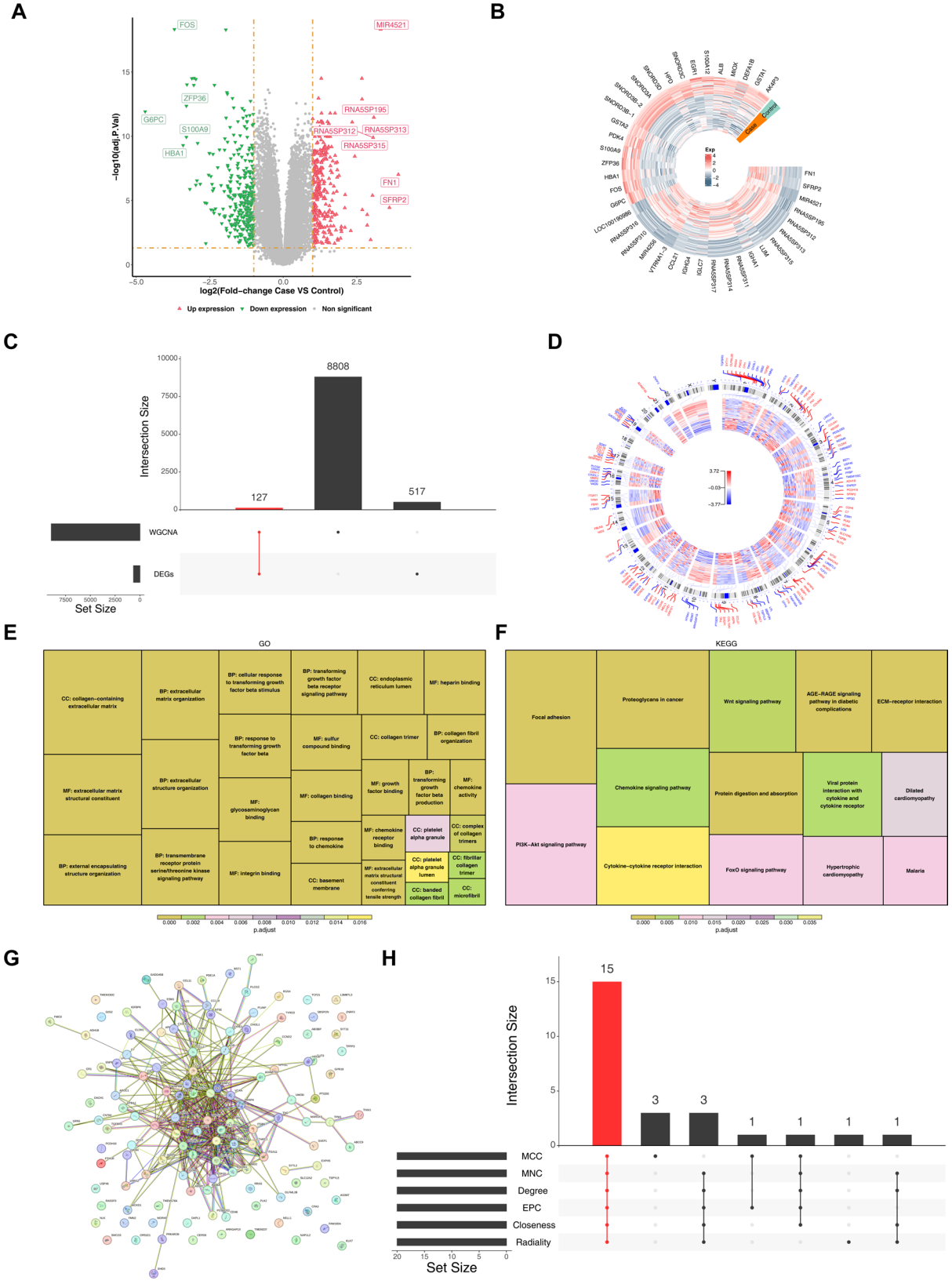

Fig. 2 Differentially expressed gene (DEG) identification of DN and enrichment analysis. **A-B**. Identification of DEGs between case and control samples. **C**. Overlap of DEGs between case and control groups with module genes (DE-MRGs). **D**.The distribution of all DE-MRGs in autosomes. **E-F**. GO (**E**), KEGG (**F**) enrichment landscape of the DE-MRGs. **G**. The PPI network of the DE-MRGs constructed using the STRING online tool.**H**.Fifteen candidate genes identified by six algorithms from Cytoscape's cytoHubba plugin

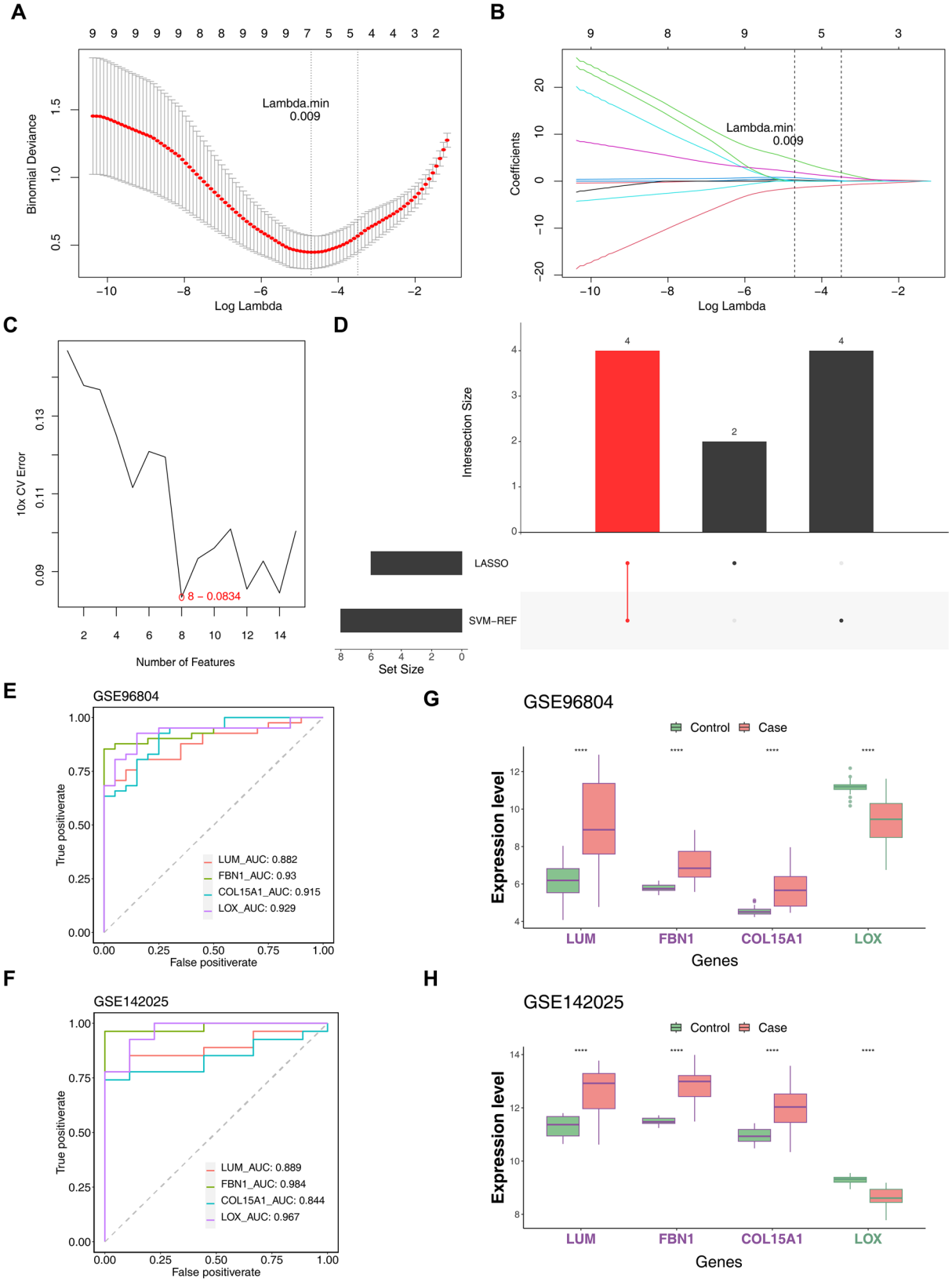

Fig. 3 (See legend on next page.)

(See figure on previous page.)

Fig. 3 Employed machine learning algorithms to scan for key genes in DN. **A-B**. Least operator shrinkage and selection operator (LASSO) logistic regression was used to screen key genes. **C**. Identification of eight feature genes based on the point where the SVM-RFE model error was lowest. **D**. Upset diagram showing the intersection feature variables filtered by the the two machine learning techniques.**E-F** Receiver operating characteristic (ROC) curves assessing the diagnostic efficacy of four key genes in the GSE96804 and GSE142025 datasets.**G-H** Analysis of the expression of four key genes based on the GSE96804 and GSE142025 datasets

intervention with streptozotocin, the blood glucose of rats in the DN group increased dramatically (Fig. 7C). Staining outcomes from kidneys pathology sections revealed that the glomeruli of the control group were morphologically structured and aligned, yet the glomeruli of the DN group were hardened and chaotic, with an increase in inflammatory cells (Fig. 7D). Finally, with the exception of *LOX*, qRT-PCR outcomes for the other three key genes agreed with the dataset's general trend (Fig. 7E).

Discussion

Diabetic nephropathy (DN) represents one of the most prevalent and severe chronic microvascular complications associated with diabetes, characterized by excessive extracellular matrix (ECM) accumulation that results in basement membrane thickening, mesangial expansion, and interstitial fibrosis within renal tubules [29]. Recent investigations have highlighted the significant role of macrophages in the initiation and progression of DN. Elevated glucose levels and advanced glycation end products (AGEs) have been shown to enhance the expression of adhesion molecules, cytokines, and chemokines in renal podocytes, mesangial cells, and epithelial cells, thereby facilitating the recruitment and activation of macrophages [30]. The activation of both resident and infiltrating macrophages within the context of DN may exacerbate inflammatory processes and contribute to fibrosis in both the glomeruli and interstitium [31]. Renal biopsies obtained from patients have consistently demonstrated the presence of macrophages within the interstitium and glomeruli at various stages of DN [12]. The pathophysiological mechanisms of DN are complex and heterogeneous [32], current research on the mechanisms by which macrophages influence DN is still incomplete, and many studies have focused on cases where the disease has already progressed to later stages Therefore, this study aims to investigate the key macrophage genes related to diabetic nephropathy, explore their underlying mechanisms, and provide clues for the early clinical diagnosis and intervention strategies of diabetic nephropathy.

Our findings revealed that the levels of neutrophils, M2 macrophages, and Th1 cells were significantly elevated in the control group compared to the DN group, while other immune cells and scores exhibited the opposite trend. Specifically, M1 macrophages were significantly elevated in the case group, while M2 macrophages were much lower. This observation aligns with previous research indicating that M1 macrophages are recruited to the renal tissue during the initial phases of DN, corroborating the assertion that the M1/M2 macrophage ratio peaks at earlier stages of the disease [33]. Functional enrichment analysis via Gene Ontology (GO) highlighted that DEMRGs were predominantly associated with chemokine receptor binding, extracellular matrix organization, and response to transforming growth factor β (TGF-β). The chemokine stromal cell-derived factor-1 can bind to its receptor, affecting the progression of DN [34]. It is well known that extracellular matrix accumulation-induced tubular interstitial fibrosis is one of the pathological features of DN [35]. Meanwhile, activation of the TGF-β signaling pathway can lead to increased proliferation of renal cells and enhanced extracellular matrix synthesis, subsequently resulting in glomerulosclerosis and tubular interstitial fibrosis [36]. In KEGG analysis, 14 functional pathways were identified as enriched, including the AGE-RAGE signaling pathway in diabetic complications and PI3K-Akt signaling pathway, both of which have been validated as critical in DN. These pathways instigate a cascade of inflammatory responses and oxidative stress, adversely affecting renal cell functionality and thereby facilitating the development of DN [37, 38]. This indicated that the DEGs related to macrophages may influence the onset and progression of DN by participating in the aforementioned pathways.

By constructing a protein interaction network and combining multiple screening methods such as LASSO and SVM-RFE, as well as various algorithms, we identified the key genes for this study: LUM, FBN1, COL15A1, and LOX. The mean AUC values all exceeded 0.8, indicating good predictive efficacy. Among them, Lumican (LUM) is a structural and functional component of the extracellular matrix (ECM) and belongs to leucine-rich proteoglycans [39]. Previous studies have shown that in human renal tubular epithelial cells cultured under high glucose conditions, the expression level of LUM increases, suggesting that it may be involved in the fibrosis process of diabetic nephropathy (DN) [40]. The single-cell analysis in this study further revealed that LUM is significantly upregulated in fibroblasts, suggesting that it may regulate the phenotype and function of fibroblasts to promote the progression of kidney fibrosis. Additionally, LUM also plays an important role in immune cell infiltration. The study found that its expression level is significantly positively correlated with the infiltration degree of macrophages (especially M1-type macrophages).

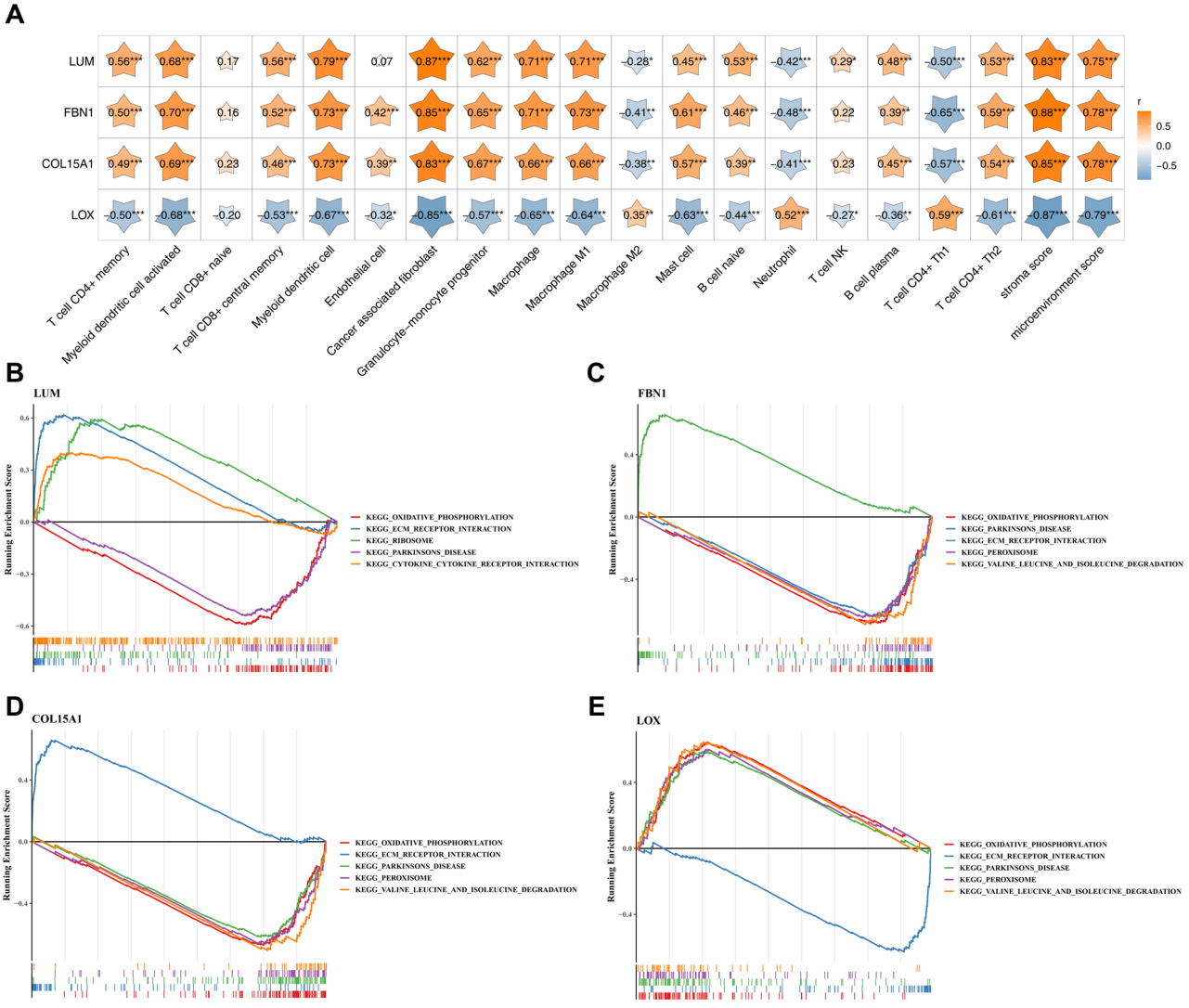

Fig. 4 Correlation analysis and GSEA enrichment analysis of the key genes. **A**. Correlation analysis between differential immune cells and key genes. **B-E**. The GSEA enrichment analysis was used to predict the KEGG downstream pathway of key genes.

Research literature indicates that the co-stimulation of LUM and LPS can promote the activation of primary macrophages and drive their polarization towards the M1-like phenotype [41], suggesting that LUM may regulate the chemotaxis, activation, and polarization processes of macrophages, enhancing the local inflammatory response in the kidney, and thereby promoting the development of diabetic nephropathy.

The gene encoding Collagen Alpha-1(XV) chain (COL15A1) is responsible for synthesizing the α-chain of type XV collagen, predominantly produced by mesenchymal-derived cells. While type XV collagen is dispersed across various tissues, its expression is most pronounced in the basement membrane region [42]. The enrichment of collagen COL15A1 can lead to the remodeling of the ECM, resulting in ECM fibrosis [43]. Such alterations in the ECM components within renal tissue may contribute to an increase in both the thickness of the glomerular basement membrane and interstitial fibrosis within renal tubules. Additionally, COL15A1 may participate in inflammation and immune regulation, potentially affecting the infiltration and activation of inflammatory cells in kidney tissue, where chronic inflammation is often associated with DN [44].

Fibrillin (FBN1) is a glycoprotein of the ECM that acts as a structural element of calcium-binding microfibrils, playing a crucial role in maintaining structural integrity in both elastic and non-elastic connective tissues throughout the organism [45]. The aberrant expression of FBN1 has been associated with the development of various human diseases, such as cancer, cardiovascular disorders, and renal diseases [45]. Earlier research employing proteomic analysis of ECM proteins in fibrotic kidneys demonstrated a significant upregulation of FBN1

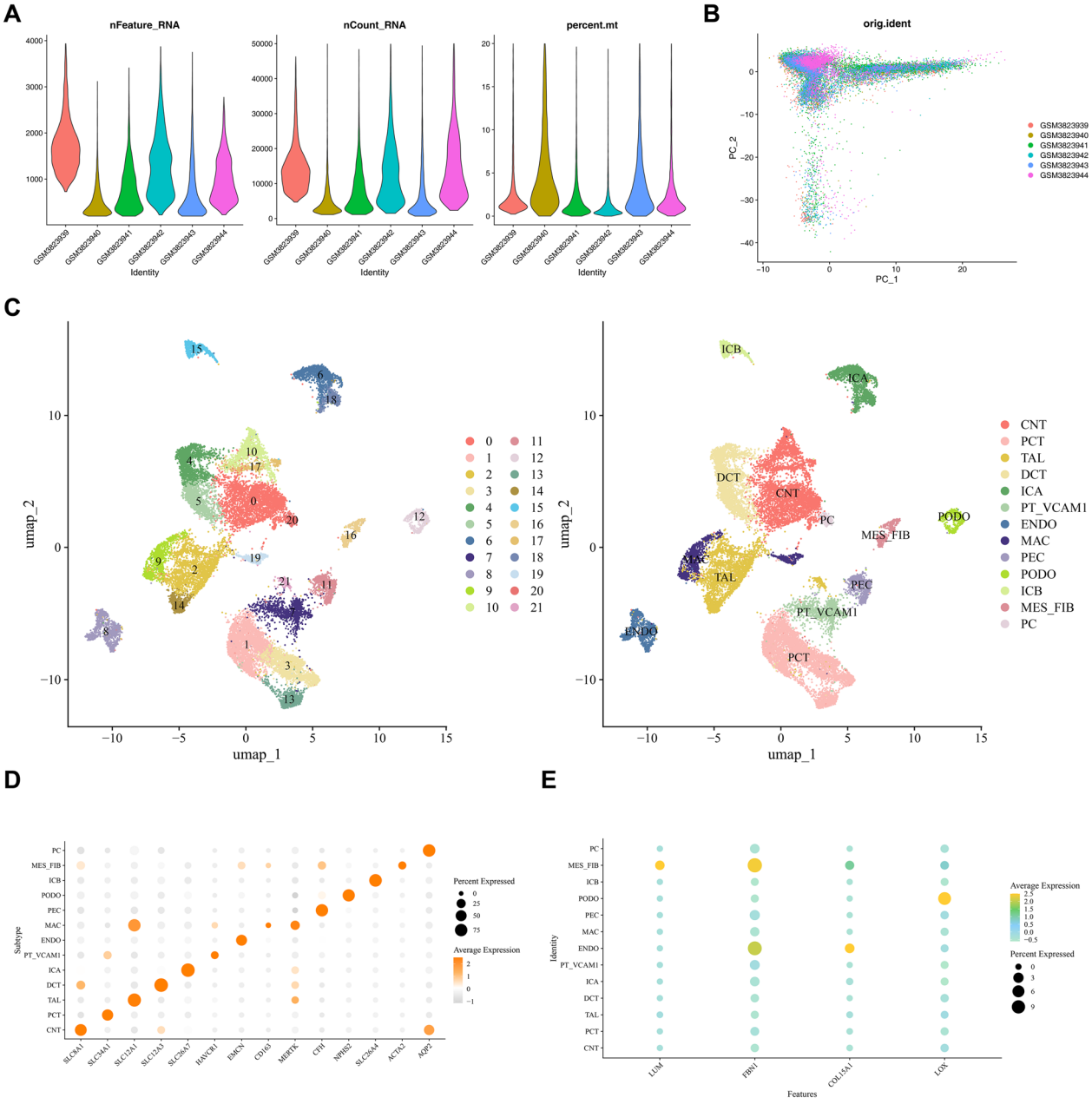

Fig. 5 Identification of 13 cell populations in the DN using scRNA-seq. **A**. Following data normalization and filtering to eliminate low-quality cells and genes, a total of 25,733 genes and 22,667 cells were detected. **B**. PCA dimensionality reduction showed no outliers or abnormal cells. **C-D**. All samples were classified into 22 clusters after UMAP clustering, which comprised 13 cell populations based on marker gene expression. **E**. Expression analysis of key genes in distinct cell populations

in decellularized kidney tissue scaffolds derived from chronic kidney disease (CKD) patients. This observation indicates that FBN1 is a major component of the fibrotic microenvironment in diseased kidneys [46]. In gastric cancer samples, elevated FBN1 expression was shown to activate the TGF-β1 and PI3K/Akt signaling pathways, thereby promoting cell proliferation and tumor advancement [47]. Although FBN1 does not directly interact with TGF-β, it is involved in regulating TGF-β activity [48]. The aforementioned studies align with the outcomes of the current study, suggesting that FBN1 may be an important factor contributing to fibrogenesis in DN.

Lysyl oxidase (LOX), a member of the LOX family, is pivotal in catalyzing reactions necessary for ECM assembly [49]. A study found that serum LOX levels in patients with renal fibrosis were higher than those in patients without renal fibrosis, and both serum and tissue LOX levels were associated with the presence and extent of renal fibrosis in CKD patients [50]. A recent study revealed that serum LOX levels were significantly

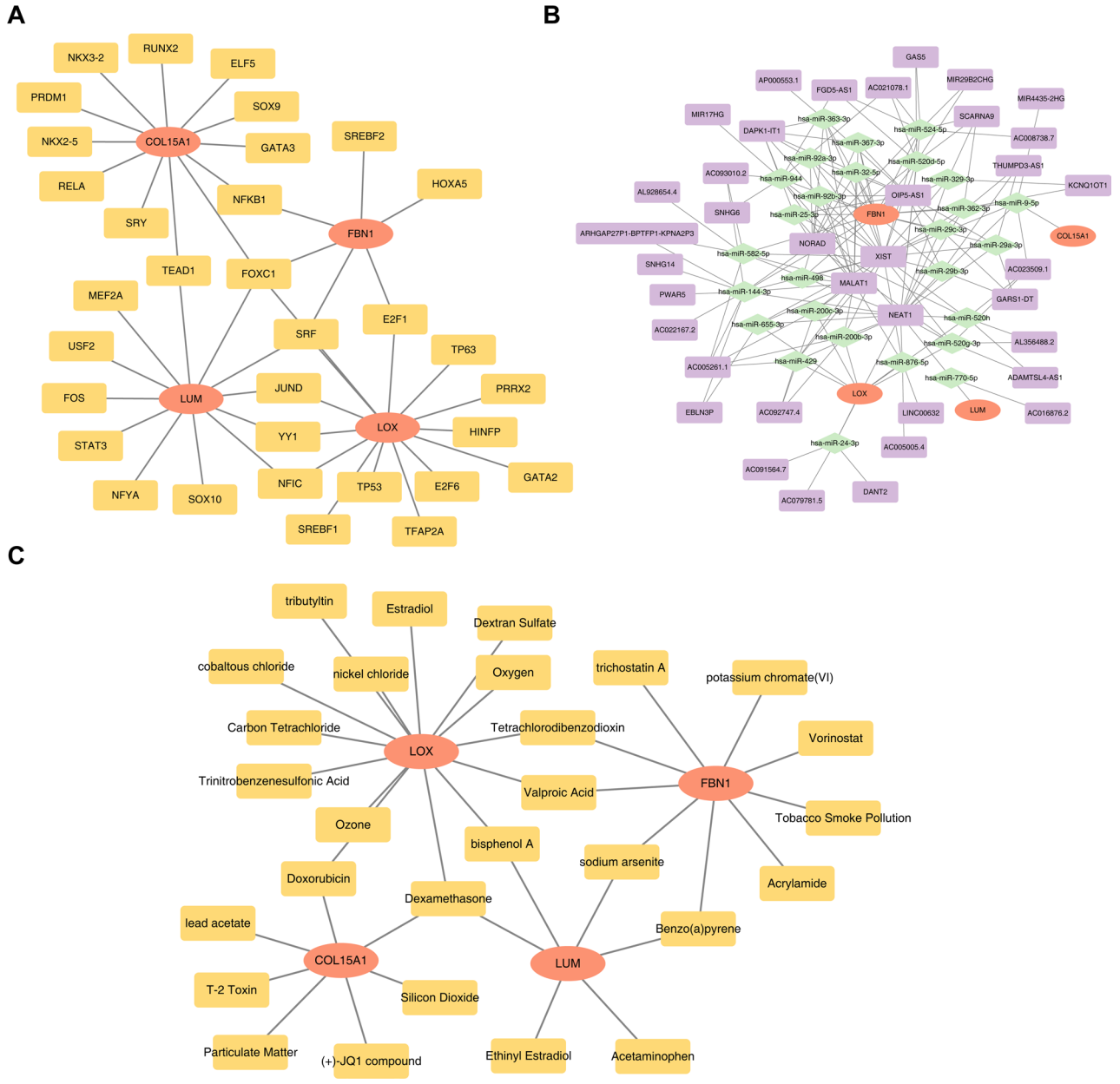

Fig. 6 Construction of related regulatory networks. **A**. Identified the transcription factors (TFs) that regulates four key genes. **B**. Construction of ceRNA network, which included 37 lncRNAs, 27 miRNAs, and 4 key genes. **C**. Recognized the chemicals in the CTD database which may either enhance the expression of LOX or reduce the expression of FBN1, COL15A1, and LUM

elevated in cases of diabetes and DN, positively correlating with blood glucose status and negatively correlating with estimated glomerular filtration rate (eGFR). It is worth noting that this study further revealed through single-cell analysis that LOX is highly expressed in podocytes, suggesting that it may play a specific role in the function of podocytes [51]. We speculate that LOX may mediate ECM cross-linking to alter the mechanical properties and permeability of the glomerular basement membrane, affecting the adhesion and morphology maintenance of podocytes, and thereby leading to dysfunction of the filtration barrier [52, 53]. However, this causal relationship still needs to be further verified.

It is essential to highlight that any bioinformatics analysis must undergo validation through experimental methods. Thus, we constructed a spontaneous DN model. RT-qPCR results indicated that the mRNA expression levels of LUM, FBN1, and COL15A1 in the kidneys of DN model rats were elevated to the control group, aligning with the findings from bioinformatics analysis and signifying that these three key genes merit additional exploration. However, the expression of the LOX gene

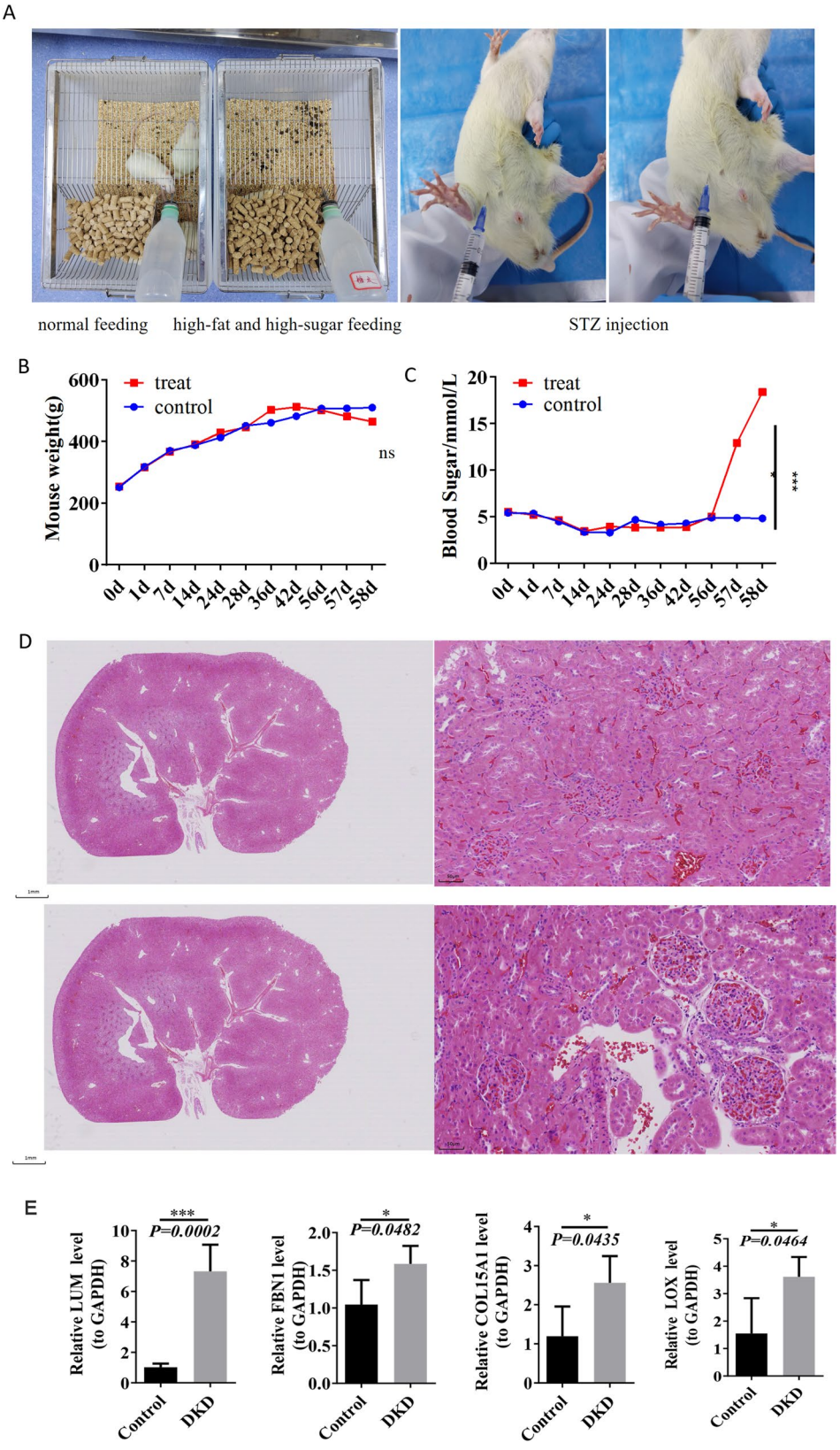

Fig. 7 Validation of key genes in animal experiments. **A**. Created a DN rat model to detect the expression of key genes. **B-C**. Changes in body weight and blood glucose in model and control groups. **D**. Staining outcomes of kidneys pathology sections. **E**. The expression levels of LUM, FBN1, COL15A1 and LOX were detected by RTssssss-qPCR

showed an increasing trend in the DN model rats, which was inconsistent with the results of bioinformatics analysis. This difference may be due to various reasons. Firstly, the expression of LOX may have a phased characteristic. The rat model induced by STZ used in this study is an acute, severe hyperglycemia model, aiming to quickly simulate the late characteristics of DN, while the samples in the human GEO dataset used in the study cover the patient groups with DN from early to late stages, with a more gradual and heterogeneous pathological process. LOX may be upregulated as a repair response in the early stage or acute injury period of the disease to promote extracellular matrix (ECM) cross-linking and maintain tissue integrity [53, 54]; while in the chronic, late fibrosis stage, the continuous abnormal remodeling of ECM may lead to its feedback downregulation. Secondly, species differences may also be an important factor causing the inconsistent results. The rat model and humans may have essential differences in gene regulation and pathological responses. Therefore, future studies need to combine longitudinal clinical cohort studies to dynamically monitor the association between LOX expression and the pathological progression and prognosis of DN, in order to clarify its complex role and regulatory mechanism in diabetic nephropathy.

To understand the biological functions and signaling pathways associated with pivotal genes, we conducted GSEA. The analysis revealed that these key genes are predominantly enriched in the PPAR signaling pathway, insulin signaling pathway, and the leukocyte transendothelial migration pathway.Abnormalities in the PPAR signaling pathway may affect the metabolism and inflammatory responses of kidney cells [55]. Dysregulation of the insulin signaling pathway could impair kidney cells' uptake and utilization of glucose, leading to damage under hyperglycemic conditions [56]. Additionally, the infiltration and activation of leukocytes in kidney tissue can cause damage to the glomerular basement membrane and glomerular epithelial cells, promoting the development of renal tubular interstitial fibrosis and ultimately resulting in a gradual loss of kidney function [57]. These pathways are intricately linked to the onset and progression of DN and may be modulated by the genes LUM, FBN1, COL15A1, and LOX.

We utilized XCell to quantified the relative abundance of 36 immune cell types and three scores, assessing the significance of differences between groups and the correlations with key genes. The relative abundance of 18 immune cell types and two scores exhibited significant variations between the groups ($p < 0.05$). Specifically, with the exception of M2 macrophages, neutrophils, and $CD4^+$ Th1 T cells, which were found to be more prevalent in the control group, all other immune cells and scores were diminished in the case group. Additionally, the four key genes showed strong correlations with activated myeloid dendritic cells, myeloid dendritic cells, cancer-associated fibroblasts, granulocyte-monocyte progenitors, and macrophages. Research has shown that activated myeloid dendritic cells can secrete large amounts of pro-inflammatory cytokines, such as TNF-α, which prompts endothelial cells to express adhesion molecules, thereby facilitating leukocyte infiltration. Meanwhile, IL-1β can stimulate kidney cells to produce more inflammatory mediators, exacerbating kidney damage [58, 59]. $CD4^+$T cells may overly differentiate toward Th1 or Th17 cell subpopulations, leading to a dominance of cytokines secreted by these two subpopulations, while the function of regulatory T cells (Tregs) is relatively suppressed. This imbalance in immune regulation can result in a persistent inflammatory response that cannot be effectively terminated, thus accelerating the advancement of DN [60].

To construct the molecular mechanism related to the regulation of diabetic nephropathy (DN), we predicted the transcription factors (TFs) related to key genes using the network database. A total of 33 transcription factors were identified. Among them, Forkhead Box C1 (FOXC1) acts as a key regulatory factor and affects four core genes simultaneously. Previous studies have suggested that the regulatory axis composed of IL-17, FOS, FOXC1, and HMMR may affect the development of diabetic nephropathy (DN) [61]. We speculate that in the high glucose microenvironment of DN, the transcription factor FOXC1 may be activated [62, 63], hereby regulating the expression of LUM, FBN1, COL15A1, and LOX. Among them, high expression of LUM, FBN1, and COL15A1 may jointly promote abnormal extracellular matrix accumulation and fibrosis process [40, 43, 46]; while the downregulation of LOX may damage the normal cross-linking and structural integrity of ECM [64]. These ECM disorders may further recruit and polarize macrophages through signal pathways such as AGE-RAGE, PI3K-Akt, etc., exacerbating local inflammation and oxidative stress, forming a vicious cycle, and ultimately promoting DN to progress to renal fibrosis [65–68]. However, the causal relationship between the above regulatory network and the progression of DN has not been fully clarified. Further experiments such as in vivo gene editing, cell-specific knockout/overexpression, and clinical sample verification are still needed to systematically explore the dynamic regulatory role of key genes in DN at different stages and cell types, in order to clarify their potential as early diagnostic markers or therapeutic targets.

In addition, this study screened 28 chemical substances from the CTD database that may act on key genes. Among them, dexamethasone was predicted to target LOX, COL15A1, and LUM. Previous studies have shown that dexamethasone can inhibit NF-κB and

other signaling pathways, down-regulate the transcription of inflammatory factors such as TNF-α, IL-1β, and IL-6, thereby exerting anti-inflammatory and immunomodulatory effects [69, 70]. However, long-term or high-dose use of glucocorticoids may cause metabolic disorders such as hyperglycemia, hyperlipidemia, and insulin resistance [71], and these side effects may mask its anti-inflammatory effects and even accelerate the progression of diabetic complications. It is worth noting that in addition to dexamethasone, valproic acid was also predicted to simultaneously target LOX and FBN1. Existing research has shown that valproic acid can alleviate cellular senescence in diabetic nephropathy by inhibiting the complement C5a receptor [72], improve insulin resistance in type 2 diabetic rats [73], and alleviate diabetic renal injury by inhibiting the apoptosis pathway related to endoplasmic reticulum stress [74]. These findings suggest that valproic acid may exert renal protective effects through multiple mechanisms. Future research can further focus on whether valproic acid affects the recruitment, polarization, and function of macrophages by regulating the expression of LOX and FBN1, thereby regulating the inflammatory and fibrotic processes in the kidneys, in order to provide safer and more targeted treatment strategies for diabetic nephropathy.

Although this study identified key genes (LUM, FBN1, COL15A1, and LOX) closely related to the progression of DN based on macrophage-related genes and analyzed the potential molecular mechanisms between these genes and DN, there are still some limitations.

Firstly, although this study integrated data from public databases, due to the sample size and the detailed clinical pathological information at the individual level, the analysis results have certain heterogeneity. Secondly, the core findings are based on human transcriptome data, while the animal model validation was only conducted in rats. The differences in genetic background and disease progression between species may be the reason for the inconsistency of some results. Moreover, diabetic nephropathy is essentially a highly heterogeneous disease syndrome. In this study, it was analyzed as a whole, which may simultaneously include gene signals related to the early inflammatory stage and the late fibrosis stage. Therefore, it is difficult to precisely distinguish the driving molecular events at different stages of the disease. Finally, the main conclusion of this study stems from bioinformatics analysis. The main contribution lies in providing insights into hypothesis generation and providing target clues for subsequent research, rather than direct clinical applications. Therefore, in the future, it is necessary to expand the clinical sample size, systematically include patients at different pathological stages, and integrate molecular typing information for stratified analysis to identify key molecular events driving different subtypes or progression stages of diabetes nephropathy, promoting the development of precise diagnosis and treatment for diabetes nephropathy. At the same time, longitudinal multi-omics integration analysis should be carried out to reveal the association between the expression dynamics of genes such as LUM, FBN1, COL15A1, and LOX and the disease evolution trajectory. In addition, functional experiments such as gene editing and cell co-culture in vitro and in vivo should be systematically conducted to verify the effects of these genes on the intrinsic cells and macrophage functions of the kidneys, and further combine spatial transcriptomics and other technologies to deeply analyze the regulatory network and interaction relationships of these genes in the renal microenvironment. These efforts will provide important basis for subsequent mechanism research, biomarker development, and targeted treatment strategies, promoting the clinical translation of the research findings.

Conclusion

In conclusion, through an extensive and systematic bioinformatics approach complemented by animal experimentation, we have identified LUM, FBN1, COL15A1, and LOX as pivotal macrophage-associated genes in DN. These results are expected to yield significant insights that will enhance early diagnostic and therapeutic strategies for DN.

Supplementary Information

The online version contains supplementary material available at https://doi.org/10.1186/s13098-026-02148-6.

Supplementary Material 1: Table S1.Primer sequences of key genes.

Supplementary Material 2: Table S2.After performing cell clustering on single-cell sequencing data based on UMAP, cell annotation is carried out using marker genes provided in the literature.

Supplementary Material 3: Table S3.Using miRNet to predict transcription factors (TFs) related to key genes based on the JASPAR database.

Supplementary Material 4: Table S4.Predict miRNAs and lncRNAs related to four key genes in the Starbase database.

Supplementary Material 5: Table S5. Predict compounds related to four key genes in the CTD database.

Supplementary Material 6.

Author contributions

Haijiao Wang and Li Zhang contributed to the hypothesis formulation, investigation, data collection, experimental procedures, and drafting of the manuscript.Baochang Shi and Hao Li participated in data analysis and manuscript revision.Yan Liu contributed to the drafting and critical revision of the manuscript.Lei Zhu conceived and supervised the study, contributed to study design, data interpretation, final editing, and approved the final version of the manuscript.

Funding

This research did not receive any specific grant from funding agencies in the public, commercial, or not-for-profit sectors.

Data availability
The datasets analyzed during the current study are available in the Gene Expression Omnibus (GEO) database under accession numbers GSE96804, GSE142025 and GSE131882 ([https://www.ncbi.nlm.nih.gov/gds/](https://www.ncbi.nlm.nih.gov/gds)).

Declarations

Ethics approval and consent to participate
All animal experiments were approved by the Ethics Committee of Shandong Provincial Third Hospital (ethical batch number: SYDW-SDLH-2024003). All experimental procedures were conducted in strict accordance with the Guide for the Care and Use of Laboratory Animals.This study is reported in accordance with the ARRIVE guidelines.not applicable.

Consent for publication
Not applicable.

Competing interests
The authors declare no competing interests.

Received: 23 October 2025 / Accepted: 11 March 2026
Published online: 02 April 2026

References

1. Sun H, Saeedi P, Karuranga S, et al. IDF Diabetes Atlas: Global, regional and country-level diabetes prevalence estimates for 2021 and projections for 2045. Diabetes Res Clin Pract Jan. 2022;183:109119.
2. Watanabe K, Sato E, Mishima E, et al. What's New in the Molecular Mechanisms of Diabetic Kidney Disease: Recent Advances. Int J Mol Sci Dec. 2022;29(1):570.
3. Ruiz-Ortega M, Rodrigues-Diez RR, Lavoz C, Rayego-Mateos S. Special Issue Diabetic Nephropathy: Diagnosis, Prevention and Treatment. J Clin Med Mar. 2020;17(3):813.
4. American Diabetes Association. Standards of Care in Diabetes—2023 Abridged for Primary Care Providers. Clin Diabetes 2 January. 2023;41(1):4–31.
5. Pitt B, Filippatos G, Agarwal R, et al. Cardiovascular Events with Finerenone in Kidney Disease and Type 2 Diabetes. N Engl J Med Dec. 2021;9(24):2252–63.
6. Bailey CJ, Day C, Bellary S. Renal Protection with SGLT2 Inhibitors: Effects in Acute and Chronic Kidney Disease. Curr Diab Rep. Jan; 2022;22(1):39–52.
7. Gerstein HC, Sattar N, Rosenstock J, et al. Cardiovascular and Renal Outcomes with Efpeglenatide in Type 2 Diabetes. N Engl J Med Sep. 2021;2(10):896–907.
8. Wang HY, Ding GH, Lin H, et al. Influence of doctors' perception on the diagnostic status of chronic kidney disease: results from 976 409 individuals with electronic health records in China. Clin Kidney J May. 2021;8(11):2428–36.
9. Hofherr A, Williams J, Gan LM, et al. Targeting inflammation for the treatment of diabetic kidney disease:a five-compartment mechanistic model[J]. BMC Nephrol. 2022;23(1):208.
10. Rayego-Mateos S, Morgado-Pascual JL, Opazo-Ríos L, et al. Pathogenic Pathways and Therapeutic Approaches Targeting Inflammation in Diabetic Nephropathy. Int J Mol Sci May. 2020;27(11):3798.
11. Zhou W, Liu Y, Hu Q, Zhou J, Lin H. The landscape of immune cell infiltration in the glomerulus of diabetic nephropathy: evidence based on bioinformatics. BMC Nephrol Sep. 2022;5(1):303.
12. Ma T, Li X, Zhu Y, et al. Excessive Activation of Notch Signaling in Macrophages Promote Kidney Inflammation, Fibrosis, and Necroptosis. Front Immunol Feb. 2022;25:13:835879.
13. Aran D, Hu Z, Butte AJ. xCell: digitally portraying the tissue cellular heterogeneity landscape. Genome Biol Nov. 2017;15(1):220.
14. Langfelder P, Horvath S. WGCNA: an R package for weighted correlation network analysis. BMC Bioinf Dec. 2008;29:9:559.
15. Ritchie ME, Phipson B, Wu D, et al. limma powers differential expression analyses for RNA-sequencing and microarray studies. Nucleic Acids Res Apr. 2015;20(7):e47.
16. Gustavsson EK, Zhang D, Reynolds RH et al. ggtranscript: an R package for the visualization and interpretation of transcript isoforms using ggplot2. Bioinformatics. Aug 2;38(15):3844–3846 (2022).
17. Zhao S, Guo Y, Sheng Q, Shyr Y. Advanced heat map and clustering analysis using heatmap3. Biomed Res Int. 2014;2014:986048.
18. Conway JR, Lex A, Gehlenborg N. UpSetR: an R package for the visualization of intersecting sets and their properties. Bioinf Sep. 2017;15(18):2938–40.
19. Hu Y, Yan C, Hsu CH, et al. OmicCircos: A Simple-to-Use R Package for the Circular Visualization of Multidimensional Omics Data. Cancer Inform. 2014;13:13–20.
20. Zhou RS, Zhang EX, Sun QF, et al. Integrated analysis of lncRNA-miRNA-mRNA ceRNA network in squamous cell carcinoma of tongue. BMC Cancer Aug. 2019;7(1):779.
21. Szklarczyk D, Franceschini A, Wyder S, et al. STRING v10: protein-protein interaction networks, integrated over the tree of life. Nucleic Acids Res. Jan; 2015;43(Database issue):D447–52.
22. Shannon P, Markiel A, Ozier O, et al. Cytoscape: a software environment for integrated models of biomolecular interaction networks. Genome Res Nov. 2003;13(11):2498–504.
23. Friedman J, Hastie T, Tibshirani R. Regularization Paths for Generalized Linear Models via Coordinate Descent. J Stat Softw. 2010;33(1):1–22.
24. Sanz H, Valim C, Vegas E, Oller JM, Reverter F. SVM-RFE: selection and visualization of the most relevant features through non-linear kernels. BMC Bioinf Nov. 2018;19(1):432.
25. Robin X, Turck N, Hainard A, et al. pROC: an open-source package for R and S+to analyze and compare ROC curves. BMC Bioinf Mar. 2011;17:12:77.
26. Liberzon A, Birger C, Thorvaldsdóttir H, et al. The Molecular Signatures Database (MSigDB) hallmark gene set collection. Cell Syst Dec. 2015;23(6):417–25.
27. Gribov A, Sill M, Lück S, et al. SEURAT: visual analytics for the integrated analysis of microarray data. BMC Med Genomics Jun. 2010;3:3:21.
28. Muto Y, Wilson PC, Ledru N, et al. Single cell transcriptional and chromatin accessibility profiling redefine cellular heterogeneity in the adult human kidney. Nat Commun Apr. 2021;13(1):2190.
29. Barrera-Chimal J, Jaisser F. Pathophysiologic mechanisms in diabetic kidney disease: A focus on current and future therapeutic targets. Diabetes Obes Metab Apr. 2020;22(Suppl 1):16–31.
30. Tang SCW, Yiu WH. Innate immunity in diabetic kidney disease. Nat Rev Nephrol Apr. 2020;16(4):206–22.
31. Tang PM, Nikolic-Paterson DJ, Lan HY. Macrophages: versatile players in renal inflammation and fibrosis. Nat Rev Nephrol Mar. 2019;15(3):144–58.
32. Redondo MJ, Hagopian WA, Oram R, et al. The clinical consequences of heterogeneity within and between different diabetes types. Diabetologia Oct. 2020;63(10):2040–8.
33. Zhang X, Yang Y, Zhao Y. Macrophage phenotype and its relationship with renal function in human diabetic nephropathy. PLoS One Sep. 2019;11(9):e0221991.
34. Ting KH, Yang PJ, Su SC, Tsai PY, Yang SF. Effect of SDF-1 and CXCR4 gene variants on the development of diabetic kidney disease. Int J Med Sci. Oct 28;21(14):2851–2861 (2024).
35. Loeffler I, Liebisch M, Daniel C, Amann K, Wolf G. Heterozygosity of mitogen-activated protein kinase organizer 1 ameliorates diabetic nephropathy and suppresses epithelial-to-mesenchymal transition-like changes in db/db mice. Nephrol Dial Transplant.Dec 1;32(12):2017–2034 (2017).
36. Zhang Y, Jin D, Kang X, et al. Signaling Pathways Involved in Diabetic Renal Fibrosis. Front Cell Dev Biol Jul. 2021;12:9:696542.
37. Chen J, Chen Y, Shu A, et al. Radix Rehmanniae and Corni Fructus against Diabetic Nephropathy via AGE-RAGE Signaling Pathway. J Diabetes Res Dec. 2020;2:2020:8358102.
38. Wang Y, Liu Y, Chen S, et al. The protective mechanism of Dehydromiltirone in diabetic kidney disease is revealed through network pharmacology and experimental validation. Front Pharmacol Aug. 2023;23:14:1201296.
39. Smith MM, Melrose J. Lumican, a Multifunctional Cell Instructive Biomarker Proteoglycan Has Novel Roles as a Marker of the Hypercoagulative State of Long Covid Disease. Int J Mol Sci Feb. 2024;29(5):2825.
40. Bai Y, Ma L, Deng D, et al. Title: Bioinformatic Identification of Genes Involved in Diabetic Nephropathy Fibrosis and their Clinical Relevance. Biochem Genet Aug. 2023;61(4):1567–84.
41. Barreto G, Senturk B, Colombo L, Brück O, Neidenbach P, Salzmann G, Zenobi-Wong M, Rottmar M. Lumican is upregulated in osteoarthritis and contributes to TLR4-induced pro-inflammatory activation of cartilage degradation and macrophage polarization. Osteoarthr Cartil. 2020;28(1):92–101.
42. Bretaud S, Guillon E, Karppinen SM, et al. Collagen XV, a multifaceted multiplexin present across tissues and species. Matrix Biol Plus Jan. 2020;15:100023.
43. Linssen EC, Demmers J, van Dijk CGM, et al. Extracellular matrix analysis of fibrosis: A step towards tissue engineering for urethral stricture disease. PLoS One Nov. 2023;30(11):e0294955.

44. Chen C, Xie Z, Ni Y, He Y. Screening immune-related blood biomarkers for DKD-related HCC using machine learning. Front Immunol Jan. 2024;22:15:1339373.
45. Li L, Huang J, Liu Y. The extracellular matrix glycoprotein fibrillin-1 in health and disease. Front Cell Dev Biol Jan. 2024;10:11:1302285.
46. Li L, He M, Tang X, et al. Proteomic landscape of the extracellular matrix in the fibrotic kidney. Kidney Int Jun. 2023;103(6):1063–76.
47. Wang X, Shi X, Lu H, et al. Succinylation Inhibits the Enzymatic Hydrolysis of the Extracellular Matrix Protein Fibrillin 1 and Promotes Gastric Cancer Progression. Adv Sci (Weinh). Sep; 2022;9(27):e2200546.
48. Lockhart-Cairns MP, Cain SA, Dajani R, et al. Latent TGFβ complexes are transglutaminase cross-linked to fibrillin to facilitate TGFβ activation. Matrix Biol Mar. 2022;107:24–39.
49. Laczko R, Csiszar K. Lysyl Oxidase (LOX): Functional Contributions to Signaling Pathways. Biomolecules. Jul 22;10(8):1093 (2020).
50. Zhang XQ, Li X, Zhou WQ, et al. Serum Lysyl Oxidase Is a Potential Diagnostic Biomarker for Kidney Fibrosis. Am J Nephrol. 2020;51(11):907–18.
51. Gayathri Devi D, Mangaraj M, Panda SK et al. Exploring the Role of Serum Lysyl Oxidase (LOX) Levels and LOX Gene Polymorphism (G473A) in Diabetic Nephropathy. Ind J Clin Biochem 2024,40(4),628-635.
52. Añazco C, López-Jiménez AJ, Rafi M, Vega-Montoto L, Zhang MZ, Hudson BG, Vanacore RM. Lysyl oxidase-like-2 cross-links collagen IV of glomerular basement membrane. J Biol Chem. 2016;291(50):25999–6012.
53. Liu X, Zhao Y, Gao J, Pawlyk B, Starcher B, Spencer JA, Yanagisawa H, Zuo J, Li T. Elastic fiber homeostasis requires lysyl oxidase–like 1 protein. Nat Genet. 2004;36(2):178–82.
54. Huang S, Jin Y, Zhang L, et al. PPAR gamma and PGC-1alpha activators protect against diabetic nephropathy by suppressing the inflammation and NF-kappaB activation. Nephrol (Carlton). Dec; 2024;29(12):858–72.
55. Mitrofanova A, Sosa MA, Fornoni A. Lipid mediators of insulin signaling in diabetic kidney disease. Am J Physiol Renal Physiol. Nov 1;317(5): F1241-F1252 (2019).
56. Mitrofanova A, Mallela SK, Ducasa GM, et al. SMPDL3b modulates insulin receptor signaling in diabetic kidney disease. Nat Commun Jun. 2019;19(1):2692.
57. Bai Y, Ma L, Deng D, Tian D, Liu W, Diao Z, Title. Bioinformatic Identification of Genes Involved in Diabetic Nephropathy Fibrosis and their Clinical Relevance. Biochem Genet Aug. 2023;61(4):1567–84.
58. Song S, Sun Y, Yu J. Causal relationship between 731 immune cells and the risk of diabetic nephropathy: a two-sample bidirectional Mendelian randomization study. Ren Fail. Dec; 2024;46(2):2387208.
59. Ren Y, Zhang H. The causal effect of inflammatory proteins and immune cell populations on diabetic nephropathy: evidence from Mendelian randomization. Int Urol Nephrol Aug. 2024;56(8):2769–78.
60. Han B, Bhowmick N, Qu Y, et al. FOXC1: an emerging marker and therapeutic target for cancer. Oncogene Jul. 2017;13(28):3957–63.
61. Chen C, He Y, Ni Y, Tang Z, Zhang W. Identification of crosstalk genes relating to ECM-receptor interaction genes in MASH and DN using bioinformatics and machine learning. J Cell Mol Med Mar. 2024;28(6):e18156.
62. Chen JH, Ye L, Zhu SL, Yang Y, Xu N. DNMT1-Mediated the Downregulation of FOXF1 Promotes High Glucose-induced Podocyte Damage by Regulating the miR-342-3p/E2F1 Axis. Cell Biochem Biophys. 2024;82(3):2957–75.
63. Ji L, Wang Q, Huang F, An T, Guo F, Zhao Y, Liu Y, He Y, Song Y, Qin G. FOXO1 overexpression attenuates tubulointerstitial fibrosis and apoptosis in diabetic kidneys by ameliorating oxidative injury via TXNIP-TRX. Oxidative Med Cell Longev. 2019;2019(1):3286928.
64. Rodríguez C, Martínez-González J. The role of lysyl oxidase enzymes in cardiac function and remodeling. Cells. 2019;8(12):1483.
65. Jin X, Li A, Dai Z, Li Y, Feng X, Qiu F. Resina Draconis Promotes Diabetic Wound Healing by Regulating the AGE-RAGE Pathway to Modulate Macrophage Polarization. Curr Issues Mol Biol. 2025;47(9):748.
66. Jang M, Oh SW, Lee Y, Kim JY, Ji ES, Kim P. Targeting extracellular matrix glycation to attenuate fibroblast activation. Acta Biomater. 2022;141:255–63.
67. Zhang R, Lan X, Zhu W, Wang L, Liu P, Li P. Regulation of autophagy by the PI3K-AKT pathway in Astragalus membranaceus-Cornus officinalis to ameliorate diabetic nephropathy. Front Pharmacol. 2025;16:1505637.
68. Li H, Wang Y, Chen B, Shi J. Silencing of PAQR3 suppresses extracellular matrix accumulation in high glucose-stimulated human glomerular mesangial cells via PI3K/AKT signaling pathway. Eur J Pharmacol. 2018;832:50–5.
69. Genito CJ, Eckshtain-Levi M, Piedra-Quintero ZL, Krovi SA, Kroboth A, Stiepel RT, Guerau-de-Arellano M, Bachelder EM, Ainslie KM. Dexamethasone and fumaric acid ester conjugate synergistically inhibits inflammation and NF-κB in macrophages. Bioconjug Chem. 2021;32(8):1629–40.
70. Wang Q, Xu B, Fan K, Wu J, Wang T. Inflammation suppression by dexamethasone via inhibition of CD147-mediated NF-κB pathway in collagen-induced arthritis rats. Mol Cell Biochem. 2020;473(1):63–76.
71. Araujo JE, Miguel-dos-Santos R, Macedo FN, Cunha PS, Fontes MT, Murata GM, Lauton-Santos S, Santana-Filho VJ, Silva AM, Antoniolli AR, Curi R. Effects of high doses of glucocorticoids on insulin-mediated vasodilation in the mesenteric artery of rats. PLoS ONE. 2020;15(3):e0230514.
72. Coughlan MT, Ziemann M, Laskowski A, Woodruff TM, Tan SM. Valproic acid attenuates cellular senescence in diabetic kidney disease through the inhibition of complement C5a receptors. Sci Rep. 2022;12(1):20278.
73. Khan S, Kumar S, Jena G. Valproic acid reduces insulin-resistance, fat deposition and FOXO1-mediated gluconeogenesis in type-2 diabetic rat. Biochimie. 2016;125:42–52.
74. Sun XY, Qin HJ, Zhang Z, Xu Y, Yang XC, Zhao DM, Li XN, Sun LK. Valproate attenuates diabetic nephropathy through inhibition of endoplasmic reticulum stress-induced apoptosis. Mol Med Rep. 2016;13(1):661–8.

Publisher's note